



Makale / Research Paper

The Effect of Three Dimensional Printed Infill Pattern on Structural Strength

Hilmi Saygın SUCUOĞLU, İsmail BOGREKCI, Pınar DEMİRCİOĞLU*, Aşlı GULTEKİN

*Adnan Menderes Üniversitesi Müh. Fak. Mak. Müh.Böl. 09010 Aydın/TÜRKİYE
pinar.demircioglu@adu.edu.tr

Received/Geliş: 15.05.2018

Revised/Düzeltilme: 29.06.2018

Accepted/Kabul: 04.07.2018

Abstract: The aim of this study is to analyze and obtain the impact of the infill pattern on structural strength for 3D printed objects using (Polylactic Acid) PLA material via Fused Deposition Modeling Technique (FDM). Linear, hexagonal and diamond types of infill patterns were selected to investigate as they are the most common for FDM. The tensile test specimens were created and prepared for simulation through Computer Aided Design (CAD) and analyzed with Computer Aided Engineering (CAE) methods. For the tensile test simulation; all of the specimens were prepared with 50% infill density. Shell of the specimens were created with the thickness of 0.8 mm, the structure was designed and supported with linear, diamond and hexagonal types of infill patterns. Layer heights were selected as 0.4 mm to decrease the analysis and printing time. A new type of infill pattern named as pyramid was also proposed and developed to obtain better results from the 3D printed objects. Nodal displacement was applied as 0.04 mm to specimens as 8 steps to create realistic tensile test simulation. For comparison; the key parameters for structural strength and pattern influence were obtained from the simulation results. Obtained results showed that the equivalent maximum stress is in the range between 7.6 to 68.6 MPa for the raw PLA, it is up to 112.3 MPa for diamond. The other significant observation is the stress value for the specimen with diamond infill reached 70.7 MPa that is close to Ultimate Tensile Strength (UTS) of PLA in the fifth step. It can be assumed from the results that specimens with linear, hexagonal and diamond are broken at the third or fourth steps of the tensile simulation as they were created with 50% infill density and their UTS is about 35 MPa. Range from 2 to 12 MPa occurred stress differences can be observed for each pattern between first and fifth steps. The diamond pattern shows the highest values. This can be due to a low density and infill structural shape effect. For the structural strength the patterns can be listed from high to low as Hexagonal > Linear > Diamond.

Keywords: Computer Aided Engineering, Fused Deposition Modeling Technique, Tensile Test Simulation, Polylactic Acid, 3D Printing Infill Pattern.

Üç Boyutlu Baskı Dolgu Deseninin Mukavemete Etkisi

Özet: Bu çalışmanın amacı; Ergiterek Yığıma ile Modelleme tekniğiyle (FDM-Fused Deposition Modeling), Polilaktik Asit (PLA-Polylactic Acid) malzeme kullanılarak oluşturulan dolgu geometrisinin mukavemete olan etkisinin analiz edilmesi ve kıyaslanmasıdır. Kıyaslama ve analiz için; yaygın olarak kullanılmasından dolayı doğrusal (linear), altıgen (hexagonal) ve elmas (diamond) tipi geometriler seçilmiştir. Çekme testi numuneleri Bilgisayar Destekli Tasarım (CAD-Computer Aided Design) metodları kullanarak hazırlanmış ve Bilgisayar Destekli Mühendislik (CAE-Computer Aided Engineering) yöntemleriyle analiz edilmiştir. Çekme testi simülasyonu için tüm numuneler %50 doluluk oranıyla hazırlanmıştır. Örneklerin kabuğu (shell) 0,8 mm kalınlıkta oluşturulmuştur. 3B baskı numuneleri, doğrusal, altıgen ve elmas tipi dolgu türleriyle tasarlanmış ve üretilmiştir. Analiz ve baskı süresini azaltmak için katman yükseklikleri 0,4 mm olarak seçilmiştir. Ayrıca, baskı ürünlerinden daha iyi sonuçlar alabilmek için piramit olarak adlandırılan yeni bir geometrik dolgu tipi tasarlanmıştır. Gerçekçi çekme testi simülasyonu oluşturmak için numunelere 8 adımda, 0,04 mm değerinde düğümsel (nodal) yer değiştirmeler uygulanmıştır. Mukavemete etkisi olan anahtar parametreler simülasyon sonuçlarından elde edilmiştir. Elde edilen sonuçlar; oluşan maksimum gerilimin, dökme PLA ile oluşturulan

How to cite this article

Sucuoglu, H.S., Bogrekcı, I., Demircioğlu, P., Gultekin, A., "The Effect of Three Dimensional Printed Infill Pattern on Structural Strength" El-Cezeri Journal of Science and Engineering, 2018, 5(3); 785-796.

Bu makaleye atıf yapmak için

Sucuoglu, H.S., Bogrekcı, I., Demircioğlu, P., Gultekin, A., "Üç Boyutlu Baskı Dolgu Deseninin Mukavemete Etkisi" El-Cezeri Fen ve Mühendislik Dergisi 2018, 5(3); 785-796.

numune için 7,6 ile 68,6 MPa aralığında olduğu halde, elmas dolgulu numune için 112,3 MPa'ya kadar yükseldiğini göstermiştir. Diğer bir önemli nokta olarak, elmas dolgulu numunenin stres değeri, beşinci aşamada ham malzemenin son çekme mukavemetine (UTS-Ultimate Tensile Strength) yakın olan 70,7 MPa değerine ulaşmış olmasıdır. Numunelerin %50 doluluk oranıyla üretilmesinden dolayı UTS değerleri 35 MPa olarak kabul edilerek simülasyonun üçüncü veya dördüncü basamaklarında kırıldığı sonucuna varılabilir. Oluşturulan farklı dolgu geometrilerinde; yaklaşık 2 ile 12 MPa aralıktaki gerilme farkları birinci ve beşinci adımlar arasında gözlemlenmiştir. En yüksek gerilim elmas geometri için oluşmuştur. Bu durum en düşük yoğunluk ve geometriye bağlı olarak açıklanabilir. Sonuç olarak, yapısal mukavemet değerlendirmesi (Altıgen> Doğrusal> Elmas) şeklinde elde edilmiştir.

Anahtar kelimeler: Bilgisayar Destekli Mühendislik, Ergiterek Yığılma ile Modelleme Tekniği, Çekme Testi Simülasyonu, Polilaktik Asit, 3B Baskı Dolgu Deseni

1. Introduction

Rapid prototyping (RP), additive manufacturing (AM) and three dimensional printing (3DP) are three terms that used for explanation of processes to fabricate parts, with different materials, via additive process, layer upon layer, first starting from a computer-aided design (CAD) model [1]. The first rapid prototyping term was derived in the mid-1980s [2,3]. Additive manufacturing is a term that scientific and technical communities use it as the standard term according to ASTM F42 and ISO TC261 committees ISO/ASTM 52915:2016, “Standard specification for additive manufacturing file format” and ISO/ASTM 52921:2013, “Standard terminology for additive manufacturing coordinate systems and test methodologies” official standards. Today 3D printing is the most popular term for additive manufacturing [1]. Many economists accept the adoption and usage of 3D printing as the “third industrial revolution” that following mechanization in the nineteenth century and assembly-line mass production in the twentieth century. The important points of 3D printing revolution were the creation of Fused Deposition Modeling (FDM) technique patented in 2009 that was developed by Crump in 1992 and widespread of open-source devices that create significant cost reduction for rapid prototyping [4]. Nowadays, there are many low-cost 3D printers available on the markets that have the lower prices than €2,000. These types of printers can be divided into three categories as; DIY (Do it yourself) open-source systems, fully assembled open-source and commercial systems with ready for use software [1].

Three dimensional printings a technique to produce components and assemblies of required manufacturing parts from CAD software. This technology was originally developed to produce the prototypes of final products. Manufacturing cost of prototypes has reduced considerably with recent developments through the introduction of inexpensive desktop printers [5]. Today three dimensional printing has wide range usage areas such as airplane, automobile parts. Fused Deposition Modeling manufacturing methods can be used for scaffold structures for bone tissue [6,7,8].

Three dimensional printing techniques are divided into four main manufacturing methods; Stereolithography (SLA), Laminated Object Manufacturing (LOM), Selective Laser Melting (SLM) and Fused Deposition Modeling [9,10]. Desktop 3D printers are designed especially for home, academic usage but rapidly growing in industry. Desktop 3D printers typically use acrylonitrile butadiene styrene (ABS) or polylactic acid (PLA) from thermoplastics feedstock [11].

The process of 3D printing with FDM technique consists of pushing a thermoplastic filament using an extruder element into a fusion chamber (hot end). The fused material is pushed through the tip of the hot end, and it is deposited in a controlled way. The process from the digital design to the deposition needs to transform the 3D geometry into movement commands and it is conducted with

conversion to G-codes. In the structure of FDM parts, four characteristic zones are formed as shown in Figure 1. The first deposited zone includes several solid layers that form the lower area of the outside of the piece. Next, the main body of the piece is built. The interior is built using an infill of a density and mesostructure. In the structure of printed parts, finally the solid top layers are deposited to close the exterior of the piece [12]. In FDM; “air gap” refers to the space between deposited filaments in this zone. Although in FDM, the infill percentage can be controlled, the air gap value cannot be specified, and consequently the real density value varies among printers and software [13].

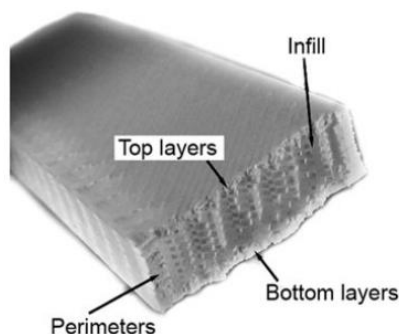


Figure 1 : Characteristic areas of printed material

2. Literature Review

There are a few studies in the literature about the impact of the FDM manufacturing parameters to mechanical behaviors and dimensional accuracy of produced parts. Rankouhi et al. studied the influence of layer thickness, infill orientations, and the number of shell perimeters for ABS mechanical characteristics. They observed that smaller layer thickness increases the strength but large air gap causes interlayer fusion bonds to fail [14]. Lanzotti et al. conducted an analysis of the influence on the dimensional accuracy when changing three deposition variables (layer thickness, deposition speed, and flow rate), and they recommended a combination of these parameters for better dimensional accuracy [15]. Afrose et al. studied the static strength and fatigue behavior of PLA material with different orientations. They obtained a 60% tensile stress of that of injection-molded PLA material [16].

3. Material and Method

In this study; the impact of the infill pattern on increase or decrease the structural strength for 3D printed objects using PLA material via Fused Deposition Modeling Technique (FDM) was analyzed. Linear, hexagonal and diamond types of infill pattern (MakerBot Z18 model desktop MakerWare Software) were selected for influence comparison. The tensile test specimens were created and prepared for simulation through CAD tools and analyzed with Computer Aided Engineering (CAE) methods.

The analysis samples for CAE analysis were printed using a MakerBot Z18 model 3D printer (MakerBot Industries, Brooklyn, USA) with 1.75 mm diameter PLA filament available through 3BFab Company. Printing parameters were specified and controlled using MakerWare Software (Figure 2).

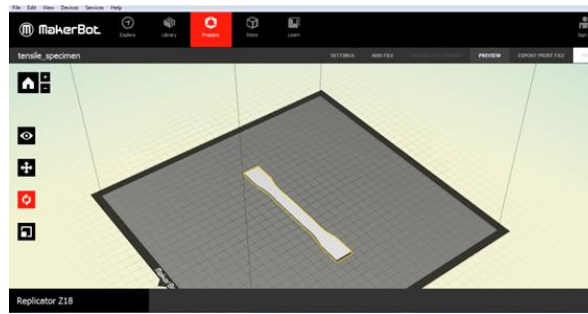


Figure 2: Creation of the analysis samples in MakerWare software

The layer thickness resolution and stepper motor positioning precision of Makerbot Z18 3D Printer are given in Table 1.

Table 1. MakerBot Replicator Z18 layer and positioning precision [17]

Layer resolution settings	(μm)
High	100
Medium	270
Low	340
Positioning Precision	
XY	11
Z	2.5

The MakerBotZ18 standard extruder is limited to manufacture the parts only with PLA material. The analysis samples were designed using a CAD software (Autodesk Inventor 2016). CAD files (ipt) were converted into a SLA file (STL) and imported into the MakerWare Software. Software was used to control the printer settings; such as layer height, percent infill, print orientation and extruder speed. Specimens with different infill patterns (linear, hexagonal and diamond) were created for analysis of pattern comparison. Models were manufactured as the half of real specimen to create detailed CAD model that include the different patterns (Figure 3).

For the tensile test simulation; all specimens were prepared with 50% infill density. Shell of the specimens were created with the thickness of 0.8 mm and structure were designed and supported with linear, hexagonal and diamond types of infill patterns. Layer heights were selected as 0.4 mm to decrease the analysis and printing time. The following control variables were also used for manufacturing;

- Extruder temperature (215 °C);
- Chamber temperature (40 °C);
- Travel speed (150 mm/s);
- Z-axis travel speed (3 mm/s);
- Print speed (90 mm/s);
- Number of shells (2).

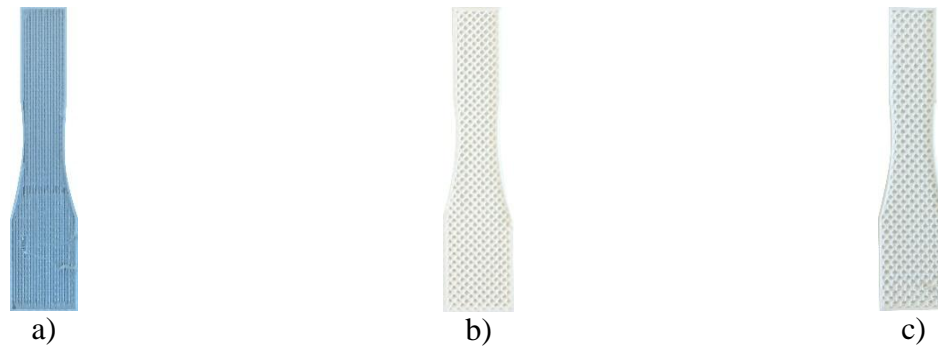


Figure 3: Manufactured specimens for pattern comparison analysis
 a) Linear b) Diamond c) Hexagonal

3.1 Design of Analysis Specimen

The dimensions and general geometry of the specimens were created according to ASTM D638–14 (Standard Test Method for Tensile Properties of Plastics). Dimensional and geometric details of the analysis test specimen are given in Figure 4 and Table 2 respectively.



Figure 4: Manufactured tensile test sample

Table 2. Dimensions of test specimen

Geometry	Dimensions (mm)
Total length (L)	113.45
Length of narrow section (LN)	33
Width of ends (W)	25
Width of narrow portion (WN)	6.2
Transition radius outside (TRO)	14
Transition radius inside (TRI)	25
Thickness (TN)	2

After one sample was manufactured for each pattern, the designs for analysis with the different patterns were created using Autodesk Inventor software with Inverse Engineering Methods (Figure 5).

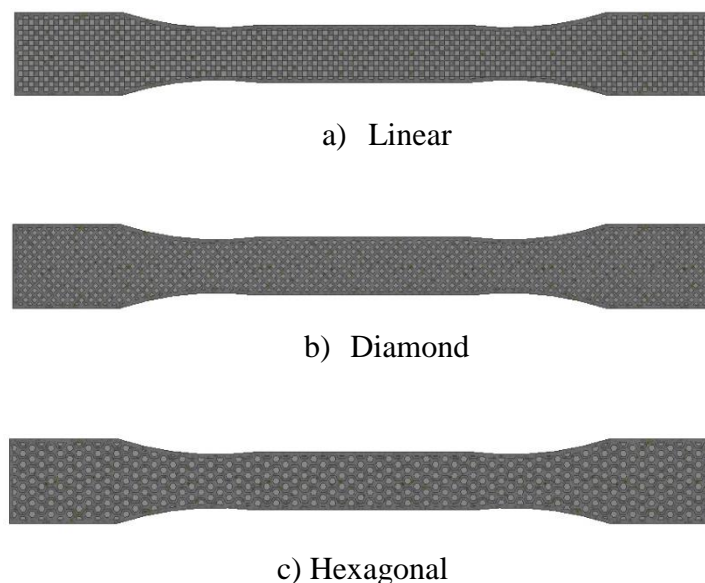


Figure 5: Designed analysis samples

3.2 Tensile Test Simulation

Tensile test simulation was conducted using Ansys Workbench Software in Static Structural analysis environment to check mechanical safety and impact of different patterns to structural strength of 3D printed parts. To create the realistic simulation environment; first the tensile test simulation was applied to specimen with raw PLA material. Material was defined to the software with physical and mechanical properties obtained from the literature (Table 3).

Table 3. Physical and mechanical properties of PLA material [18]

Characteristic	Unit	Amount
Solid density	g/cm^3	1.25
Tensile strength	MPa	59
Ultimate tensile strength	MPa	73
Young modulus	GPa	1.28
Poisson ratio	-	0.36

Body of the tensile specimen was reduced to surface to decrease the process time for numerical calculations and prevent from computational burden. Nodal displacements were applied to all created nodes with the value of 0.04 mm [1] as right and left sides to create the loading rate required for realistic tensile test simulation. Tensile test simulation was performed for 8 second with the specified loading rate value as the occurred equivalent maximum stress was reached to the UTS value (Figure 6). Analysis results were compared with stress-strain curve from the literature. As

obtained results similar with the literature the analysis set was applied to linear, hexagonal and diamond patterns.

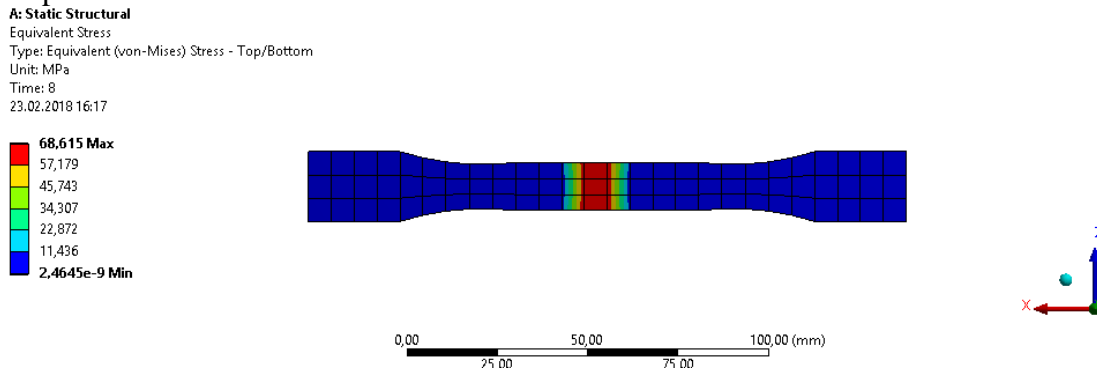


Figure 6: Tensile test simulation with Ansys Workbench Static Structural tool

3.3 Pyramid Infill

According to obtained results; a new type of infill pattern named as pyramid, manufactured with golden ratio geometry, was also proposed and developed to obtain better results from the 3D printed objects (Figure 7). The same analysis procedure was applied to specimen designed with pyramid infill.

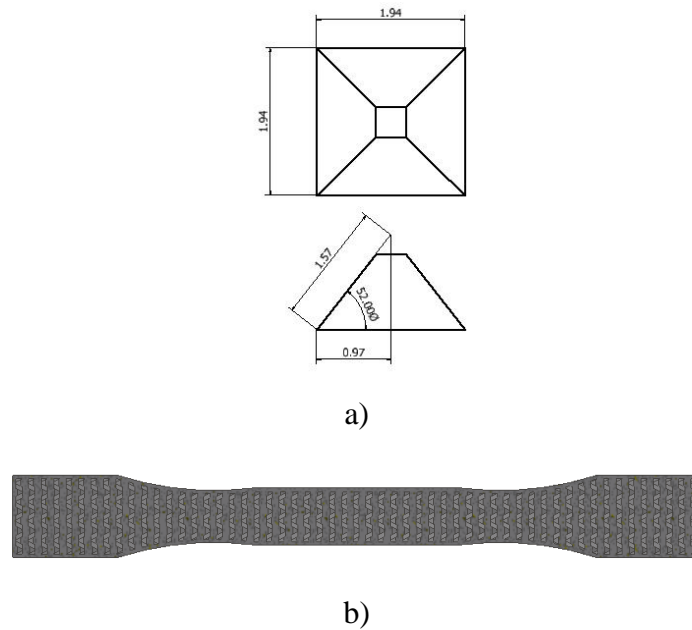


Figure 7: Pyramid infill a) Technical details b) Specimen with pyramid infill

4. Results and Discussion

4.1 Raw PLA Specimen

The stress-strain values for test specimen with raw material are given in Figure 8 and Table 4. When the results for linear zone were compared with Yang et al. study “*Mechanical Properties of Chemical Cross-Linked PLA*”, the similar values were obtained. The same simulation procedure was also applied to structural steel (St 37-2) and similar results were obtained.

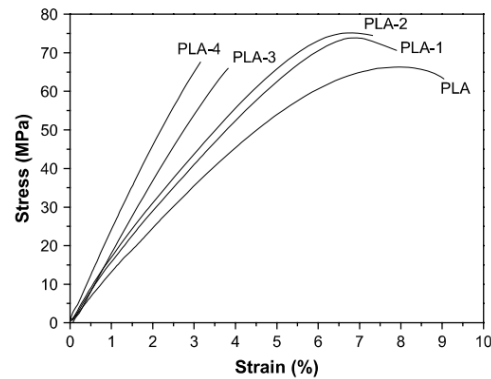


Figure 8: Yang et al. stress-strain curve [19]

Table 4. Obtained stress-strain values of raw PLA

No. of Step	Equivalent maximum stress (MPa)	Strain (%)
1	7.6	0.8
2	17.2	1.5
3	25.7	2.3
4	34.3	3.1
5	42.9	3.8
6	51.5	4.6
7	60.0	5.4
8	68.6	6.2

4.2 Raw PLA Specimen

The tensile test simulation with the same analysis set of Raw PLA was applied to different patterns. The analysis set for hexagonal pattern is shown in Figure 9.

The results obtained from the simulation show differences between the different parameters of infill density and pattern, also called mesostructures, of the specimens. As can be seen in Table 5, a higher level of density resulted in a lower amount of voids in the infill, and subsequently, lower occurred stress with applied loading rate. While the equivalent maximum stress is in the range between 7.6 to 68.6 MPa for the raw PLA, it is up to 112.3 MPa for diamond. The other significant observation is the stress value for the specimen with diamond infill reached to 70.7 MPa that is close to UTS of PLA in the fifth step. It can be assumed from the results that specimens with linear, hexagonal and diamond are broken at the third or fourth steps of the tensile simulation as they were created with 50% infill density and their UTS is about 35 MPa.

Range from 2 to 12 MPa occurred stress differences can be observed for each pattern between first and fifth steps. The similar behavior is for strain values. The diamond pattern shows the highest values. This can be due to a low density and infill structural shape effect. For the structural strength, the patterns can be classified as Hexagonal > Linear > Diamond.

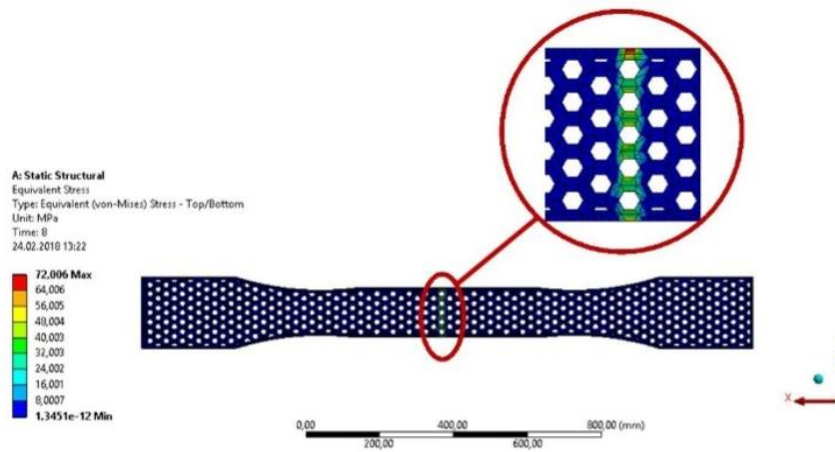


Figure 9: . Tension test simulation for hexagonal pattern

The analysis results for raw PLA, linear, diamond and hexagonal patterns are given in Table 5 for comparison.

Table 5. Comparison of Different Patterns

No. of Steps	Equivalent maximum stress (MPa)				Strain (%)			
	Raw PLA	Linear	Hexagonal	Diamond	Raw PLA	Linear	Hexagonal	Diamond
1	7.6	11.8	10.1	14.2	0.8	1.1	0.9	1.3
2	17.2	23.6	19.3	28.3	1.5	2.1	1.7	2.6
3	25.7	35.4	28.3	42.4	2.3	3.2	2.8	3.9
4	34.3	47.3	38.0	56.6	3.1	4.3	4.1	5.2
5	42.9	59.1	47.4	70.7	3.8	5.3	5.1	6.5
6	51.5	70.9	57.2	84.9	4.6	6.4	6.1	7.8
7	60.0	82.7	66.2	99.0	5.4	7.5	7.2	9.1
8	68.6	94.5	77.0	112.3	6.2	8.5	8.1	10.4

Obtained safety factor values supports the idea (Table 6).

Table 6. Safety factor comparison

Pattern type	Safety factor at fifth step
Raw PLA	1.8
Linear	0.9
Hexagonal	1.2
Diamond	0.7

These relationships may partly be explained by the slight variation of weight, geometric structure and consequently the density differences between patterns of the same virtual density as given in Table 7.

Table 7. Weight of tensile specimens with different infill patterns

Infill Type	Weight (g)
Linear	12.3
Hexagonal	14.2
Diamond	11.2

4.3 Pyramid Infill

The obtained results from tensile test simulation for diamond infill geometry are given in Table 8. New infill geometry provides better structural strength. At the last step, the stress and strain values reached to 75 MPa and this is 7.1 % lower than hexagonal. It may be explained with the geometric property of created infill pattern that provide lower amount of voids with the same infill density 50%.

Table 8. Analysis results for pyramid infill

No. of Steps	Equivalent maximum stress (MPa)	Strain (%)
1	9.12	0.8
2	18.3	1.7
3	27.4	2.5
4	36.5	3.3
5	45.6	4.2
6	54.7	5.1
7	65.9	5.8
8	75.0	7.1

4. Conclusion

In this research, the effects of infill density and pattern on mechanical properties of the FDM 3D printing process have been studied. Findings from the analyses show that:

1. The hexagonal pattern in a 50% infill showed the minimum occurred stress at all steps, with the maximum value of 77 MPa.
2. Under the same density, the hexagonal pattern had a better tensile strength; this discrepancy could be attributed to small variations of amount of plastic deposited for each pattern and geometric effect.
3. The deposition trajectory and the interlayer bonding were different for hexagonal, diamond and linear patterns. It could be a reason for the tensile strength and elasticity differences.

4. The classification among the different infill patterns related to tensile strength was; Hexagon > Linear > Diamond.
5. It can provide successful results if pyramid type of infill pattern can be assigned for manufacturing. However, more research is required to understand the different effects of the pyramid infill.
6. Further researches are planned to understand the effect of the infill pattern types, environmental conditions such as extruder temperature to mechanical behavior with the experimental studies.

References

- [1] Lanzotti, A., Grasso, M., Staiano, G., Martorelli, M. The impact of process parameters on mechanical properties of parts fabricated in PLA with an open-source 3-D printer. *Rapid Prototyping Journal*, 2015, 21(5): 604-617.
- [2] Jacobs, P.F., *Rapid prototyping & manufacturing: fundamentals of stereo-lithography*. Society of Manufacturing Engineers, ISBN-13: 978-0872634251, (1992).
- [3] Jacobs, P.F., *Stereolithography and other RP&M technologies: from rapid prototyping to rapid tooling*. Society of Manufacturing Engineers, 1995.
- [4] Huang, S. H., Liu, P., Mokasdar, A., Hou, L. Additive manufacturing and its societal impact: a literature review. *The International Journal of Advanced Manufacturing Technology*, 2013, 67(5-8): 1191-1203.
- [5] Melenka, G. W., Schofield, J. S., Dawson, M. R., Carey, J. P. Evaluation of dimensional accuracy and material properties of the MakerBot 3D desktop printer. *Rapid Prototyping Journal*, 2015, 21(5): 618-627.
- [6] Leigh, S. J., Bradley, R. J., Pursell, C. P., Billson, D. R., Hutchins, D. A. A simple, low-cost conductive composite material for 3D printing of electronic sensors. *PloS one*, 2012, 7(11), e49365.
- [7] Melchels, F. P., Feijen, J., Grijpma, D. W. A review on stereolithography and its applications in biomedical engineering. *Biomaterials*, 2010, 31(24): 6121-6130.
- [8] Mäkitie, A. A., Korpela, J., Elomaa, L., et. al. Novel additive manufactured scaffolds for tissue engineered trachea research. *Acta Oto-Laryngologica*, 2013, 133(4): 412-417.
- [9] Chua, C.K., Leong, K.F., Lim, C.S., *Rapid prototyping: principles and applications (Vol1)*. World Scientific, (2003).
- [10] Novakova-Marcincinova, L., Novak-Marcincin, J. Verification of mechanical properties of abs materials used in FDM rapid prototyping technology. *Proceedings in manufacturing systems*, 2003, 8(2): 87-92.
- [11] Williams, C. B., Cochran, J. K., Rosen, D. W. Additive manufacturing of metallic cellular materials via three-dimensional printing. *The Int. J. of Advanced Manufacturing Technology*, 2011, 53(1-4): 231-239.
- [12] Fernandez-Vicente, M., Calle, W., Ferrandiz, S., Conejero, A. Effect of infill parameters on tensile mechanical behavior in desktop 3D printing. *3D printing and additive manufacturing*, 2016, 3(3): 183-192.
- [13] Tymrak, B. M., Kreiger, M., Pearce, J. M. Mechanical properties of components fabricated with open-source 3-D printers under realistic environmental conditions. *Materials & Design*, 2016, 58: 242-246.
- [14] Rankouhi, B., Javadpour, S., Delfanian, F., Letcher, T. Failure analysis and mechanical characterization of 3D printed ABS with respect to layer thickness and orientation. *Journal of Failure Analysis and Prevention*, 2016, 16(3): 467-481.
- [15] Lanzotti, A., Martorelli, M., Staiano, G. Understanding process parameter effects of

- reprap open-source three-dimensional printers through a design of experiments approach. *Journal of Manufacturing Science and Engineering*, 2015, 137(1): 011017
- [16] Afrose, M. F., Masood, S. H., Iovenitti, P., Nikzad, M., Sarsi, I. Effects of part build orientations on fatigue behaviour of FDM-processed PLA material. *Progress in Additive Manufacturing*. 2016, 1(1-2): 21-28.
- [17] MakerBot; *MakerBotZ18 Desktop 3D Printer User Manual*, MakerBot, 2018
- [18] Farah, S., Anderson, D. G., Langer, R. Physical and mechanical properties of PLA, and their functions in widespread applications-A comprehensive review. *Advanced drug delivery reviews*, 2016, 107: 367-392.
- [19] Yang, S. L., Wu, Z. H., Yang, W., Yang, M.B., Thermal and mechanical properties of chemical crosslinked polylactide (PLA). *Polymer Testing*, 2008, 27(8): 957-963.